Asociación Argentina
de Mecánica Computacional

Mecánica Computacional Vol XXIX, págs. 4361-4375 (artículo completo)
Eduardo Dvorkin, Marcela Goldschmit, Mario Storti (Eds.)
Buenos Aires, Argentina, 15-18 Noviembre 2010

SEMI-ANALYTICAL BENCHMARK SOLUTIONS OF THICK PLATES IN BENDING

Tales de V. Lisbôa and Rogério J. Marczak

Grupo de Mecânica Aplicada, Universidade Federal do Rio Grande do Sul, Rua Sarmento Leite, 435 90050-170 Porto Alegre – RS, Brasil, taleslisboa@yahoo.com.br, www-gmap.mecanica.ufrgs.br

Keyword: thick plates, semi-analytical solutions, bending, *pb-2*

Abstract. The modified Rayleigh-Ritz method (*pb-2*) is applied to obtain solutions for moderately thick plates under transverse constant load. Using Mindlin's plate theory, a semi-analytical approach is used to generate displacement solutions for several boundary conditions. A convergence study is presented to validate the results, which are discussed and compared with similar solutions from literature. The method can be used to generate new benchmark solutions for validation and practical applications.

Copyright © 2010 Asociación Argentina de Mecánica Computacional http://www.amcaonline.org.ar

1. INTRODUCTION

Several tools to solve differential equations numerically by approximating the exact/analytical solution have been developed in the recent years. This is a response for the crescent improvement in computers hardware. Consequently, many research which were unfeasible before have become attractive, directing resources of R&D for those areas. Advances have been obtained in merging efficient numerical tools and powerful computational resources. However, some approximate solutions provided by these numerical methodologies no longer explain certain phenomena. Thus, the study of analytical solutions of the differential equations which govern these phenomena is important to calibrate new numerical tools and verify the numerical results already obtained.

Among the structural theories that describe the behavior of two-dimensional plane problems, bending of plates considering the transverse shear strain (also called thick plates theories) are the ones which most lack analytical solutions. Considering that, designers may compare their numerical results to other structural theories, like three-dimensional elasticity, whenever possible. This can lead to significant errors because the differential equations are different and the boundary conditions are incompatible. Therefore, analytical solutions for the theories that describe the plate behavior are important for the development of benchmarks, as well as calibration of numerical tools and results.

The derivation of analytical solutions for general cases is, however, a very complex subject. Depending on the differential equations and the boundary conditions, these solutions may not exist. Thus these solutions are restricted to simply cases and/or academic problems. For the cases where the solution is nonexistent or very difficult to obtain, semi-analytical solutions are an interesting alternative. Their formulation considers some types of variables approximation and numerical integration. However, differently from numerical results, these solutions are functions of initial parameters and fully satisfy the boundary conditions.

Many researches published papers with numerical and analytical solutions for thick plate theories. Salerno and Goldberg (1960) were the first to obtain solutions for thick plates. Using Reissner's plate theory, they derived analytical solutions for Lévy plates under constant transversal load. Using the finite difference method, Craig (1987) obtained numerical solutions for Reissner's plate theory. The researcher explored the case in which a concentrated load is applied on the center of the plate and shows that the out-plane shear strain can be significant even when the plate is thin. Kant and Hinton (1983) used the Segmentation Method to obtain numerical results for Mindlin plates. The boundary conditions were based in Lévy plates. More recently, Lee et. al. (2002) obtained analytical solutions for Lévy plates using relationships between classical and Mindlin plates theories. Their solutions were based on series expansion of hyperbolic and trigonometric functions. Therefore, due a characteristic of Lévy solution and the nature of trigonometric functions, these solutions did not show full symmetry in cases with symmetric loads and boundary conditions. Following the same way, Wang et. al. (2001) related Mindlin's plate theory with Reissner's plate theory getting analytical solutions for the last. Again, the authors used the same type of interpolation series and the fully symmetry of the solution can not be achieved.

The aim of this paper is obtain semi-analytical solutions for thick plates with several boundary conditions. A modified Rayleigh-Ritz method, called *pb-2*, is used to derive the differential equations of Mindlin's plate theory. The modification of the method simplifies the application of the boundary conditions in the interpolation functions. These are the same in both directions to avoid non-symmetric solutions, as verified in Lee et. al. (2002) and Wang et. al. (2001). A convergence study is performed and the obtained solutions are discussed and compared with the available literature.

Copyright © 2010 Asociación Argentina de Mecánica Computacional http://www.amcaonline.org.ar

The *pb-2* method has been used previously in several plate problems. Kitipornchai et. al. (1994) applied this method to obtain the dynamic solution for thick trapezoidal plates under several boundary conditions. Wang et. al. (1997) used the method to obtain stress resultants on corner supported rectangular plates. Singh and Elaghabash (2003) used this methodology to get numerical solutions for finite displacement on thin plates. Similar ideas will be used herein.

2. MATHEMATICAL MODEL

The displacement field of Mindlin's plate theory, described by Mindlin (1951), can be shown as:

$$\begin{aligned} U_\alpha(x_1,x_2,x_3) &= -x_3\phi_\alpha(x_1,x_2) \\ U_3(x_1,x_2,x_3) &= u_3(x_1,x_2) \end{aligned} \tag{1}$$

where U_α, U_3 and u_3 are the longitudinal, transverse and out-plane displacements, respectively. ϕ_α are the rotations normal to the coordinate axis. Greek indices vary from 1 to 2 and repeated indices denote summation unless otherwise noted. As shown on the equation (1), in-plane displacements will be not considerate. The material behavior is assumed to be isotropic and linear.

The infinitesimal strain tensor $(\boldsymbol{\varepsilon})$ can be described as:

$$\begin{aligned} 2\varepsilon_{\alpha\beta} &= -x_3\left(\phi_{\alpha,\beta}+\phi_{\beta,\alpha}\right) \\ 2\varepsilon_{\alpha 3} &= u_{3,\alpha}-\phi_\alpha \end{aligned} \tag{2}$$

where the $\varepsilon_{\alpha\beta}$ are the in-plane strain, $\varepsilon_{\alpha 3}$ are the out-plane strain, or transverse shear strain, and the comma in the subscript denotes differentiation. The Cauchy stress tensor $(\boldsymbol{\sigma})$ can be obtained using the generalized Hooke's law and the equation (2) resulting in:

$$\begin{aligned} \sigma_{\alpha\beta} &= -x_3 G\left[\phi_{\alpha,\beta}+\phi_{\beta,\alpha}+\frac{\nu}{2(1-\nu)}\phi_{\gamma,\gamma}\delta_{\alpha\beta}\right] \\ \sigma_{\alpha 3} &= \kappa^2 G\left(u_{3,\alpha}-\phi_\alpha\right) \end{aligned} \tag{3}$$

where G is the transverse elastic modulus, ν is the Poisson coefficient , $\delta_{\alpha\beta}$ is the Kronecker delta function and κ^2 is the conventional transverse shear correction.

The resultant stress can be obtained integrating the Cauchy stress tensor through the thickness, resulting in:

$$\begin{aligned} N_{\alpha\beta} &= 0 \\ M_{\alpha\beta} &= -D(1-\nu)\left[\phi_{\alpha,\beta}+\phi_{\beta,\alpha}+\frac{\nu}{2(1-\nu)}\phi_{\gamma,\gamma}\delta_{\alpha\beta}\right] \\ Q_\alpha &= \kappa^2 Gh\left(u_{3,\alpha}-\phi_\alpha\right) \end{aligned} \tag{4}$$

where $N_{\alpha\beta}$ are the normal $(\alpha=\beta)$ and in-plane shear resultant stress $(\alpha\neq\beta)$, $M_{\alpha\beta}$ are the bending $(\alpha=\beta)$ and twisting $(\alpha\neq\beta)$ moments and Q_α are the out-plane shear resultant stress. The bending stiffness, known as Sophie-German constant, is given by

Copyright © 2010 Asociación Argentina de Mecánica Computacional http://www.amcaonline.org.ar

$D = Gh^3/6(1-\nu)$. Disregarding the in-plane displacement, expressed in equation (1), the normal and in-plane shear resultant stress are null, as shown in equation (4).

The Rayleigh-Ritz method (RR) is based on the Minimal Potential Energy Principle (MPEP). This principle shows that the equilibrium of the structure from all possible equilibrium positions is that one which corresponds to the minimum state of energy. Mathematically:

$$\delta\Pi = \delta(U - V_e) \tag{5}$$

where U is the total strain energy, V_e is the external work and Π is the potential energy functional.

The interpolation functions that approximate the displacement field shown in the equation (1) will be constructed in the following way:

$$\begin{aligned} u_3 &\cong \hat{u}_3 = g_3 \mathbf{c}_3 \cdot \boldsymbol{\theta}_3 \\ \phi_1 &\cong \hat{\phi}_1 = g_4 \mathbf{c}_4 \cdot \boldsymbol{\theta}_4 \\ \phi_2 &\cong \hat{\phi}_2 = g_5 \mathbf{c}_5 \cdot \boldsymbol{\theta}_5 \end{aligned} \tag{6}$$

where the circumflex upper script denotes approximation, $\mathbf{c}_3$, $\mathbf{c}_4$ and $\mathbf{c}_5$ are the weights of the interpolation functions ($\boldsymbol{\theta}_3$, $\boldsymbol{\theta}_4$ and $\boldsymbol{\theta}_5$).The dot product between the vectors represents the linear combination of the interpolation functions. The scalars g_3, g_3 and g_3 obey the relationship shown as:

$$g_i = \prod_{k=1}^{n} \left(x_j - x_{cc}\right)^{\delta_{cc}} \tag{7}$$

where x_{cc} is the position of the boundary condition in function of the coordinate axis x_j, δ_{cc} is the type of boundary condition applied and n is the number of boundary conditions in respect of the coordinate axis considered (subscript *j*).

δ_{cc} value	u_3	ϕ_n	ϕ_t
Clamped	1	1	1
Simply supported	1	1	0
Free	0	0	0

Table 1: value for each boundary condition

Equation (7) is the aforementioned modification of the RR method. It will be shown that equation inserts zeros in the interpolation functions where the kinematic boundary conditions must be satisfied. Therefore the interpolation functions ($\boldsymbol{\theta}_3$,$\boldsymbol{\theta}_4$and $\boldsymbol{\theta}_5$) do not need to be kinematically admissible from the outset, which is a requirement and a difficulty in the original RR method. The difference $\left(x_j - x_{cc}\right)$ represents the equation of boundary lines of the plate. The exponent δ_{cc} can assume two values, associated to the type of boundary condition: 0 for free and 1 for fixed edges, where fixed means no displacement and/or rotation, depending on the degree of freedom (DOF). It is clear that when δ_{cc} is equal to 1, a zero is inserted in the interpolation functions at the position of $x_j = x_{cc}$. The composition of the

Copyright © 2010 Asociación Argentina de Mecánica Computacional http://www.amcaonline.org.ar

values of δ_{cc} for each DOF constructs a complete boundary condition. Table 1 shows the type of the boundary condition with respect to the δ_{cc} value for each DOF.

The interpolation space chosen is a polynomial one. This is due the fact that the equation (7) belongs to this space andintegrations can be done exactly with Gaussian Quadrature.Then, the functions that will be interpolated the displacement field can be described as:

$$\theta_j^m = x_1^i x_2^{ng-i} \tag{8}$$

where ng is the degree of the primary polynomial (degree of the interpolation functions before the imposition of the boundary conditions) and

$$m = \frac{(ng+1)(ng+2)}{2} - i \tag{9}$$

where the superscript m identifies the position of the function in the vector of the interpolation functions. The subscript j denotes the DOF. As shown in the equation (8), the interpolation functions are equal for each approximated variables.

Therefore, the final number of constants for each interpolation depends uniquely on the degree of the primary polynomial (ng) and it can be calculated as:

$$nc = \frac{(ng+1)(ng+2)}{2} \tag{10}$$

3. MATRIX FORMULATION

To evaluate the energy functional expressed in equation (5), the strain energy and the external work need to be calculated. The first one is estimated by the integral of the internal product between the Cauchy stress tensor and the infinitesimal strain tensor in the plate's volume. The second one is evaluated by the integral of the dot product between the load and the displacement vector over the middle surface area of the plate. Thus, the strain energy is given by:

$$U = \frac{1}{2}\int_{\Omega} \mathbf{E}^T \mathbf{C}\mathbf{E}\, d\,\Omega \tag{11}$$

where

$$\mathbf{E} = \begin{Bmatrix} -x_3\phi_{1,1} & -x_3\phi_{2,2} & -x_3(\phi_{1,2}+\phi_{2,1}) & u_{3,1}-\phi_1 & u_{3,1}-\phi_1 \end{Bmatrix}^T$$

$$\mathbf{C} = \begin{bmatrix} \frac{2G}{1-\nu} & \frac{2\nu G}{1-\nu} & 0 & 0 & 0 \\ \frac{2\nu G}{1-\nu} & \frac{2G}{1-\nu} & 0 & 0 & 0 \\ 0 & 0 & G & 0 & 0 \\ 0 & 0 & 0 & \kappa^2 G & 0 \\ 0 & 0 & 0 & 0 & \kappa^2 G \end{bmatrix} \tag{12}$$

and Ω is the plate volume. The vector $\mathbf{E}$ can be decomposed as:

$$\mathbf{E} = \mathbf{H}\xi \tag{13}$$

Copyright © 2010 Asociación Argentina de Mecánica Computacional http://www.amcaonline.org.ar

where

$$\begin{aligned}\boldsymbol{\xi} &= \left\{\phi_{1,1} \quad \phi_{2,2} \quad \phi_{1,2}+\phi_{2,1} \quad u_{3,1}-\phi_1 \quad u_{3,2}-\phi_2\right\}^T \\ \mathbf{H} &= diag\left\langle -x_3, -x_3, -x_3, 1, 1\right\rangle\end{aligned} \tag{14}$$

The vector expressed in the first equation of (14) can be written in terms of displacement and rotations applying a linear operator described as:

$$\mathbf{D}_L = \begin{bmatrix} 0 & \partial\cdot/\partial x_1 & 0 \\ 0 & 0 & \partial\cdot/\partial x_2 \\ 0 & \partial\cdot/\partial x_2 & \partial\cdot/\partial x_1 \\ \partial\cdot/\partial x_1 & 1 & 0 \\ \partial\cdot/\partial x_2 & 0 & 1 \end{bmatrix} \tag{15}$$

Then, the first equation of (14) can be expressed by:

$$\boldsymbol{\xi} = \mathbf{D}_L \boldsymbol{\Delta} \tag{16}$$

where $\boldsymbol{\Delta} = \left\{u_3 \quad \phi_1 \quad \phi_2\right\}^T$. With the interpolation described in equation (6), that expression can be written as:

$$\hat{\boldsymbol{\Delta}} = \begin{Bmatrix} \hat{u}_3 \\ \hat{\phi}_1 \\ \hat{\phi}_2 \end{Bmatrix} = \begin{bmatrix} g_3 & 0 & 0 \\ 0 & g_4 & 0 \\ 0 & 0 & g_5 \end{bmatrix} \begin{bmatrix} \boldsymbol{\theta}_3^T & 0 & 0 \\ 0 & \boldsymbol{\theta}_4^T & 0 \\ 0 & 0 & \boldsymbol{\theta}_5^T \end{bmatrix} \begin{Bmatrix} \mathbf{c}_3 \\ \mathbf{c}_4 \\ \mathbf{c}_5 \end{Bmatrix} = \boldsymbol{\Lambda}\mathbf{N}\boldsymbol{\lambda} \tag{17}$$

Therefore:

$$\begin{aligned} \boldsymbol{\Lambda} &= diag\left\langle g_3, g_4, g_5\right\rangle \\ \mathbf{N} &= \begin{bmatrix} \boldsymbol{\theta}_3^T & 0 & 0 \\ 0 & \boldsymbol{\theta}_4^T & 0 \\ 0 & 0 & \boldsymbol{\theta}_5^T \end{bmatrix} \\ \boldsymbol{\lambda} &= \left\{\mathbf{c}_3 \quad \mathbf{c}_4 \quad \mathbf{c}_5\right\}^T \end{aligned} \tag{18}$$

After all modifications, the equation (11) can be rewritten as:

$$U = \frac{1}{2}\int_{\Omega} \boldsymbol{\lambda}^T \mathbf{N}^T \boldsymbol{\Lambda} \mathbf{D}_L^T \mathbf{H}^T \mathbf{C} \mathbf{H} \mathbf{D}_L \boldsymbol{\Lambda} \mathbf{N} \boldsymbol{\lambda}\, d\,\Omega \tag{19}$$

The external work is calculated as:

$$V_e = \int_A \boldsymbol{\Delta}^T \mathbf{P}\, dA = \int_A \boldsymbol{\lambda}^T \mathbf{N}^T \boldsymbol{\Lambda} \mathbf{P}\, dA \tag{20}$$

where $\mathbf{P} = \left\{q_0 \quad m_1 \quad m_2\right\}$, q_0 is the transverse load, m_1 and m_2 are the distributed moments applied on the plate's middle surface.

The first variation of total potential energy can be written, in function of vector $\boldsymbol{\lambda}$ as:

Copyright © 2010 Asociación Argentina de Mecánica Computacional http://www.amcaonline.org.ar

$$\delta\Pi = \delta\left(U - V_e\right) = \frac{dU}{d\boldsymbol{\lambda}} - \frac{dV_e}{d\boldsymbol{\lambda}} \tag{21}$$

Through the equations (19) – (20), the right part of the equation (21) is derived resulting in:

$$\int_A \mathbf{N}^T \boldsymbol{\Lambda}\mathbf{D}_L^T \mathbf{H}^T \mathbf{C}\mathbf{H}\mathbf{D}_L \boldsymbol{\Lambda}\mathbf{N} dA\boldsymbol{\lambda} - \int_A \mathbf{N}^T \boldsymbol{\Lambda}\mathbf{P} dA = 0 \tag{22}$$

After the matrix products and the integration are carried out, the vector $\boldsymbol{\lambda}$ can be obtained. Thus, the equation (22) is rewritten as:

$$\int_A \mathbf{B}_L^T \mathbf{R}_L \mathbf{B}_L dA\boldsymbol{\lambda} = \int_A \mathbf{N}^T \boldsymbol{\Lambda}\mathbf{P} dA \tag{23}$$

where:

$$\mathbf{B}_L = \mathbf{D}_L \boldsymbol{\Lambda}\mathbf{N}$$

$$\mathbf{R}_L = \int_{-\frac{h}{2}}^{+\frac{h}{2}} \mathbf{H}^T \mathbf{C}\mathbf{H} dx_3 = \begin{bmatrix} \frac{Gh^3}{6(1-\nu)} & \frac{Gh^3}{6(1-\nu)} & 0 & 0 & 0 \\ \frac{\nu Gh^3}{6(1-\nu)} & \frac{\nu Gh^3}{6(1-\nu)} & 0 & 0 & 0 \\ 0 & 0 & \frac{Gh^3}{12} & 0 & 0 \\ 0 & 0 & 0 & G\kappa^2 h & 0 \\ 0 & 0 & 0 & 0 & G\kappa^2 h \end{bmatrix} \tag{24}$$

4. PARAMETERIZATION

Several system variables were parameterized to simplify the comparisons and to improve numerical stability.

The load vector $\mathbf{P}$ was parameterized as:

$$q_1 = \frac{q_0 a^4}{Gh^4} \tag{25}$$

As can be seen, the matrix $\mathbf{R}_L$ expressed in the second part of equation (24) depends linearly on G. Thus, it is simple to understand why q_1 depends inversely on G: the response of the linear system, described in equation (23), using this parameterization, is independent to transverse shear modulus.

The geometry of the plate was parameterized like the four-node finite element. The linear system expressed in equation (23), with these parameterizations, is modified as:

$$\boldsymbol{\lambda} = q_1 \eta^4 \left[\int_{-1}^{1}\int_{-1}^{1} \mathbf{B}_L^T \breve{\mathbf{R}}_L \mathbf{B}_L \left|\mathbf{J}\right| ds_1 ds_2 \right]^{-1} \int_{-1}^{1}\int_{-1}^{-1} \mathbf{N}^T \boldsymbol{\Lambda}\breve{\mathbf{P}} \left|\mathbf{J}\right| ds_1 ds_2 \tag{26}$$

where:

$$\begin{aligned} \eta &= h/a \\ \breve{\mathbf{P}} &= \{1 \quad 0 \quad 0\} \end{aligned} \tag{27}$$

Copyright © 2010 Asociación Argentina de Mecánica Computacional http://www.amcaonline.org.ar

and $\breve{\mathbf{R}}_L = \mathbf{R}_L / G$, s_1 and s_2 are the natural coordinates of the parameterized plate and $|\mathbf{J}|$ is the determinant of the Jacobian matrix of the coordinate transformation. The integrals are carried out with the Gaussian Quadrature.

The out-plane displacement, u_3, have two dimensionless parameters:

$$\begin{aligned} \overline{w}_1 &= wD \Big/ q_0 a^4 \\ \overline{w}_2 &= \overline{w}_1 \Big/ w_c \end{aligned} \tag{28}$$

where w is the central transverse displacement and $\overline{w}_c$ is a convergence value.

5. RESULTS

Before show the semi-analytical solutions, numerical results are presented to verify the methodology convergence. Four types of boundary conditions were analyzed and seven different thicknesses were tested. Thus, three aspect ratio (a/b) were utilized. Varying these three parameters, the convergence was tested in 84 different cases.

The boundary conditions utilized in this work were SSSS, CCCC, SCSC and SFSF where S, C and F denote simply supported, clamped and free edge, respectively. The tested thicknesses were 0.001, 0.01, 0.05, 0.1, 0.15, 0.2 and 0.25. Both thick and thin plates were analyzed, considering these values. The three aspect ratio used were 1, 2 and 5.

The convergence study was accomplished in order to estimate the value of *ng* which could deliver accurate results. From this study was observed that SSSS, SFSF and SCSC plates need only odd values of *ng*. Even values produced similar results for all variables like displacement/rotations and stress resultants than the odd immediately below. In case of CCCC plates, the convergence was incremented only for even values of *ng*. Therefore, only even values of *ng* were used for CCCC plates and odd values of *ng* for the other boundary conditions.

To exemplify the methodology convergence, two cases are plotted in Figure 1, differing in boundary conditions. Figure 2 shows the convergence of SSSS plates with different aspect ratios. It is noted, in both figures, that the aspect ratio and the thickness affects the convergence. It is observed is all boundary conditions.

The center displacement values obtained for SSSS plates using this methodology is presented in Table 2. These results were compared to other solutions found in the literature and a good agreement was achieved. Although the interpolation methods usually show a significant degradation in stress values when compared to displacement/rotation values, in this type of boundary conditions the numerical results of moment and transverse shear stress resultant were also in a good agreement with the solutions in literature, as shown in Table 3.

Differing from classical plate theory, the displacement is dependent of the plate's thickness. However, the center of the plate when the thickness tends to zero corresponds to the solution of the classical plate theory. Another interesting point is the results obtained by Lee et. al. (2002) and Wang et. al. (2001). As shown in Table 3, the solution of these authors have a clear lack of symmetry Q_1 and Q_2. This is due the fact that the interpolation functions utilized by these authors symmetric, demanding a huge number of terms to achieve the fully symmetry of the stress resultants. The results obtained in the present methodology were fully symmetric as shown in Table 3.

Copyright © 2010 Asociación Argentina de Mecánica Computacional http://www.amcaonline.org.ar

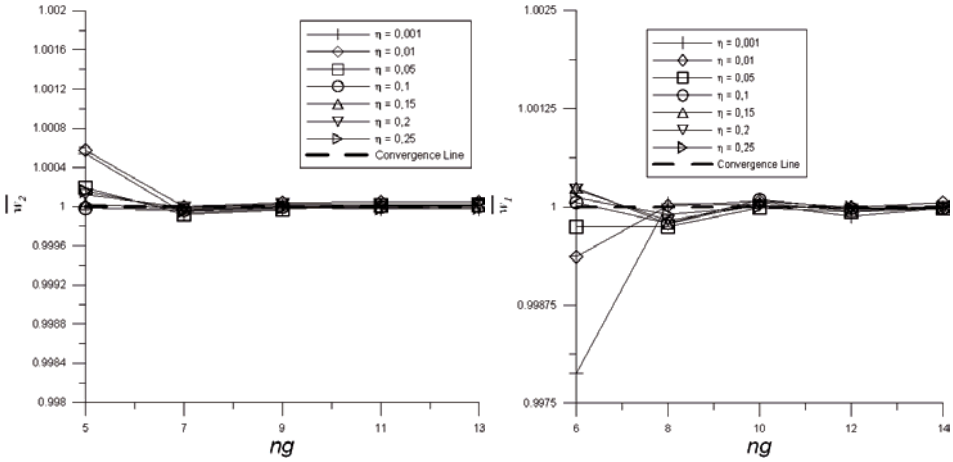

Figure 1 - Convergence curves of square plates: (a) SFSF (b) CCCC

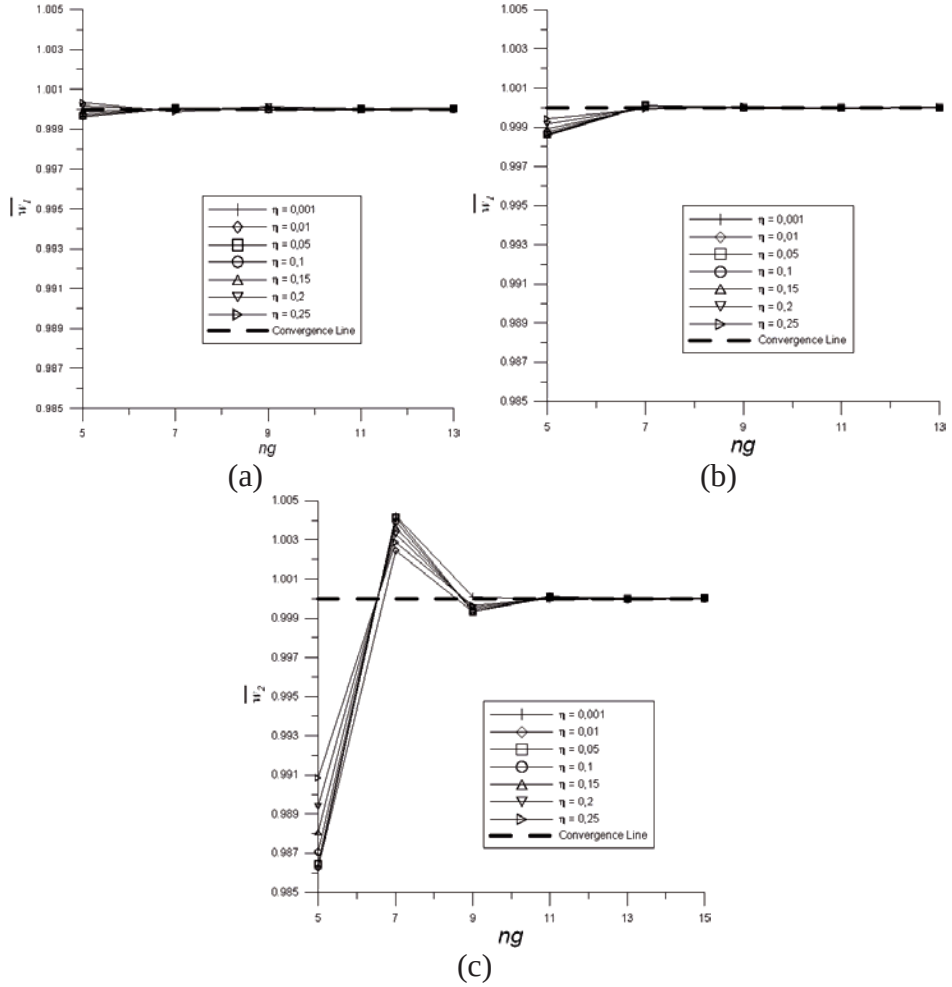

Figure 2 - Convergence curves for SSSS plates with aspect ratio: (a) 1 (b) 2 and (c) 5

Copyright © 2010 Asociación Argentina de Mecánica Computacional http://www.amcaonline.org.ar

η	$b/a=1$			$b/a=2$			$b/a=5$		
	Present Work	Lee et. al. (2002)	Salerno & Goldberg (1960)	Present Work	Lee et. al. (2002)	Salerno & Goldberg (1960)	Present Work	Lee et. al. (2002)	Salerno & Goldberg (1960)
0.001	0.0040624	-	-	0.010129	-	-	0.012971	-	-
0.010	0.0040625	0.00406	0.00406	0.010132	0.01013	0.01013	0.012974	0.01297	0.01297
0.050	0.0041149	0.00411	0.00411	0.010210	0.01021	0.01020	0.013060	0.01306	0.01305
0.100	0.0042728	0.00427	0.00424	0.010454	0.01045	0.01041	0.013328	0.01333	0.01327
0.150	0.0045360	0.00454	0.00446	0.010861	0.01086	0.01075	0.013774	0.01377	0.01365
0.200	0.0049040	0.00490	0.00478	0.011430	0.01143	0.01123	0.014398	0.01440	0.01418
0.250	0.0053778	-	-	0.012162	-	-	0.015201	-	-

Table 2 - Center displacement of SSSS plates

η	$M_{11}(s_1=0,s_2=0)$			$M_{22}(s_1=0,s_2=0)$			$M_{12}(s_1=0,s_2=0)$		
	Present Work	Lee et. al. (2002)	Wang et. al. (2001)	Present Work	Lee et. al. (2002)	Wang et. al. (2001)	Present Work	Lee et. al. (2002)	Wang et. al. (2001)
CPT		0.0479			0.0479			0.0325	
0.001	0.0478	0.0479	0.0479	0.0478	0.0479	0.0479	0.0324	0.0325	0.0325
0.010	0.0478	0.0479	0.0479	0.0478	0.0479	0.0479	0.0324	0.0325	0.0325
0.050	0.0478	0.0479	0.0480	0.0478	0.0479	0.0480	0.0324	0.0325	0.0322
0.100	0.0478	0.0479	0.0482	0.0478	0.0479	0.0482	0.0324	0.0325	0.0316
0.150	0.0478	0.0479	0.0485	0.0478	0.0479	0.0485	0.0324	0.0325	0.0304
0.200	0.0478	0.0479	0.0491	0.0478	0.0479	0.0491	0.0324	0.0325	0.0288
0.250	0.0478	-	-	0.0478	-	-	0.0324	-	-

η	$Q_1(s_1=-1,s_2=0)$			$Q_2(s_1=0,s_2=-1)$		
	Present Work	Lee et. al. (2002)	Wang et. al. (2001)	Present Work	Lee et. al. (2002)	Wang et. al. (2001)
CPT		0.333			0.0479	
0.001	0.33	0.333	0.333	0.33	0.338	0.338
0.010	0.33	0.333	0.333	0.33	0.338	0.338
0.050	0.33	0.333	0.333	0.33	0.338	0.338
0.100	0.34	0.333	0.333	0.34	0.338	0.338
0.150	0.34	0.333	0.333	0.34	0.338	0.338
0.200	0.34	0.333	0.333	0.34	0.338	0.338
0.250	0.34	-	-	0.34	-	-

Table 3 - Stress resultants of square SSSS plates

In case of SCSC plates, the results for center displacement show a good agreement when compared to other author, as shown in Table 4.

Copyright © 2010 Asociación Argentina de Mecánica Computacional http://www.amcaonline.org.ar

η	$b/a=1$			$b/a=2$			$b/a=5$		
	Present Work	Lee et. al. (2002)	Wang et. al. (2001)	Present Work	Lee et. al. (2002)	Wang et. al. (2001)	Present Work	Lee et. al. (2002)	Wang et. al. (2001)
0.001	0.0019172	-	-	0.0084451	-	-	0.012931	-	-
0.010	0.0019202	0.00192	0.00192	0.0084492	0.00845	0.00845	0.012935	0.1293	0.01293
0.050	0.0019918	0.00199	0.00199	0.0085481	0.00855	0.00854	0.013021	0.01302	0.01311
0.100	0.0022087	0.00221	0.00202	0.0088500	0.00885	0.00882	0.01329	0.01329	0.01338
0.150	0.0025558	0.00256	0.00254	0.0093379	0.00934	0.00926	0.01374	0.01374	0.01382
0.200	0.0030211	0.00302	0.00298	0.010000	0.01000	0.00986	0.01436	0.01436	0.01445
0.250	0.0035957	-	-	0.010827	-	-	0.01517	-	-

Table 4 - Center displacement of SCSC plates

Analytical solutions for fully clamped plate (CCCC) are notable rare than the other type of boundary conditions. The results obtained with the present methodology were compared with the excellent work of Taylor and Govindjee (2002) for thin fully clamped plates, in Table 5. In order to obtain 10 accurate digits, Taylor and Govindjee (2002) solved a matrix system with 2000x2000. The values obtained by the present method were generated from a system of 315x315, using *ng* equal to 13. Interestingly, the results for thin plates $\eta = 0.001$ point out for an error in the third digit of the classical solution of Timoshenko and Woinowski-Krieger.

η	$b/a=1$		$b/a=2$	
	Present Work	Taylor & Govindjee (2002)	Present Work	Taylor & Govindjee (2002)
0.001	0.0012654	0.001265319036	0.0025330	0.002532955769
0.010	0.0012678	-	0.002608	-
0.100	0.0015046	-	0.002962	-
0.250	0.0026580	-	0.004837	-

Table 5 - Center displacement of CCCC plates

For SFSF plates, the Table 6 shows the results of center displacement and at the middle of the free edge for square plates. It is noted that the both results corresponds to the values found in the literature. The Figure 2 illustrates a contour plot of the normalized transverse displacement and the normalized bending moment for a plate with $b/a = 5$ and are plotted in normalized space. This aspect ratio is used to evidence the anti-clasticcurvature which appears in this type of boundary conditions. It can be noted that the methodology presented here captures this effect.

η	Center of the plate			Middle of the free edge		
	Present Work	Lee et. al. (2002)	Wang et. al. (2001)	Present Work	Lee et. al. (2002)	Wang et. al. (2001)
0.001	0.013094	-	-	0.015011	-	-
0.010	0.013097	-	-	0.015023	-	-
0.050	0.013187	-	-	0.015214	-	-
0.100	0.013459	0.01346	0.01341	0.015600	0.01560	0.01557
0.150	0.013910	0.01391	0.01379	0.016161	0.01616	0.01609
0.200	0.014539	0.01454	0.01433	0.016898	0.01690	0.01678
0.250	0.015347	0.01536	0.01502	0.017809	0.01781	0.01762

Table 6 - Displacement on the center and in the middle of the free edge in SFSF square plates

Copyright © 2010 Asociación Argentina de Mecánica Computacional http://www.amcaonline.org.ar

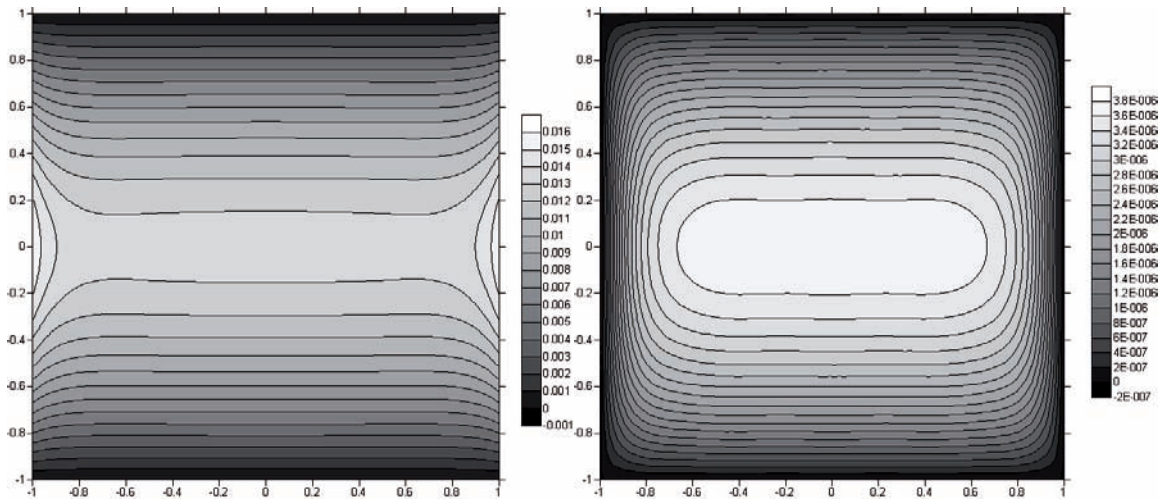

(a) (b)

Figure 3 - (a) $\overline{w}_1$ and (b) M_{11} in SFSF plates in normalized coordinates

6. PARAMETRIC SOLUTIONS FOR BENCHMARK

A study on the influence of the plate's thickness over the displacement was carried out using the presented methodology. This is not necessary in the CPT since the differential equations are insensitive to thickness. On other hand, in analysis of thick plates, this influence is significant because it is the parameter which controls the transverse shear deformation. Due the high memory requirements to deal with symbolic expressions, the degree of the primary polynomial (ng) used is 5 for SSSS, SFSF and SCSC and 6 for CCCC boundary conditions. The central displacement field was approximated with a polynomial expression of fifth degree:

$$w = \frac{q_0 a^4}{D} \sum_{i=1}^{6} a_i \eta^{i-1} \tag{29}$$

andthe independent constants are expressed by the Table 7.

	r	a_1	a_2	a_3	a_4	a_5	a_6
SSSS	1.00	0.004061	0	0.02110	0	0	0
	1.35	0.006742	0	0.02698	0	0	0
	1.65	0.008573	0	0.03020	0	0	0
	2.00	0.010110	0	0.03260	0	0	0
CCCC	1.00	0.00126	0.00008	0.02431	-0.00949	-0.01561	0.06569
	1.35	0.00199	0.00033	0.02666	0.03017	-0.10755	0.27689
	1.65	0.00233	0.00077	0.02344	0.07749	-0.31589	0.44471
	2.00	0.00249	0.00131	0.02069	0.09141	-0.29759	0.35772
SFSF	1.00	0.01310	-0.00060	0.04480	-0.04402	0.07339	0
	1.35	0.04436	-0.00111	0.09605	-0.21213	0.70352	-0.91537
	1.65	0.10038	-0.00126	0.14654	-0.29543	0.86315	-1.01987
	2.00	0.21942	-0.00159	0.22572	-0.44526	1.13023	-1.15651

Copyright © 2010 Asociación Argentina de Mecánica Computacional http://www.amcaonline.org.ar

SCSC	1.00	0.00193	-0.00069	0.04341	-0.12023	0.39030	-0.53692
	1.35	0.00426	-0.00040	0.04790	-0.09195	0.27263	-0.37795
	1.65	0.00635	0.00015	0.04267	-0.04086	0.11663	-0.19000
	2.00	0.00842	0.00081	0.03791	-0.03482	0.18575	-0.35542

Table 7 - Coefficients of the equation (29) for each aspect ratio and boundary conditions

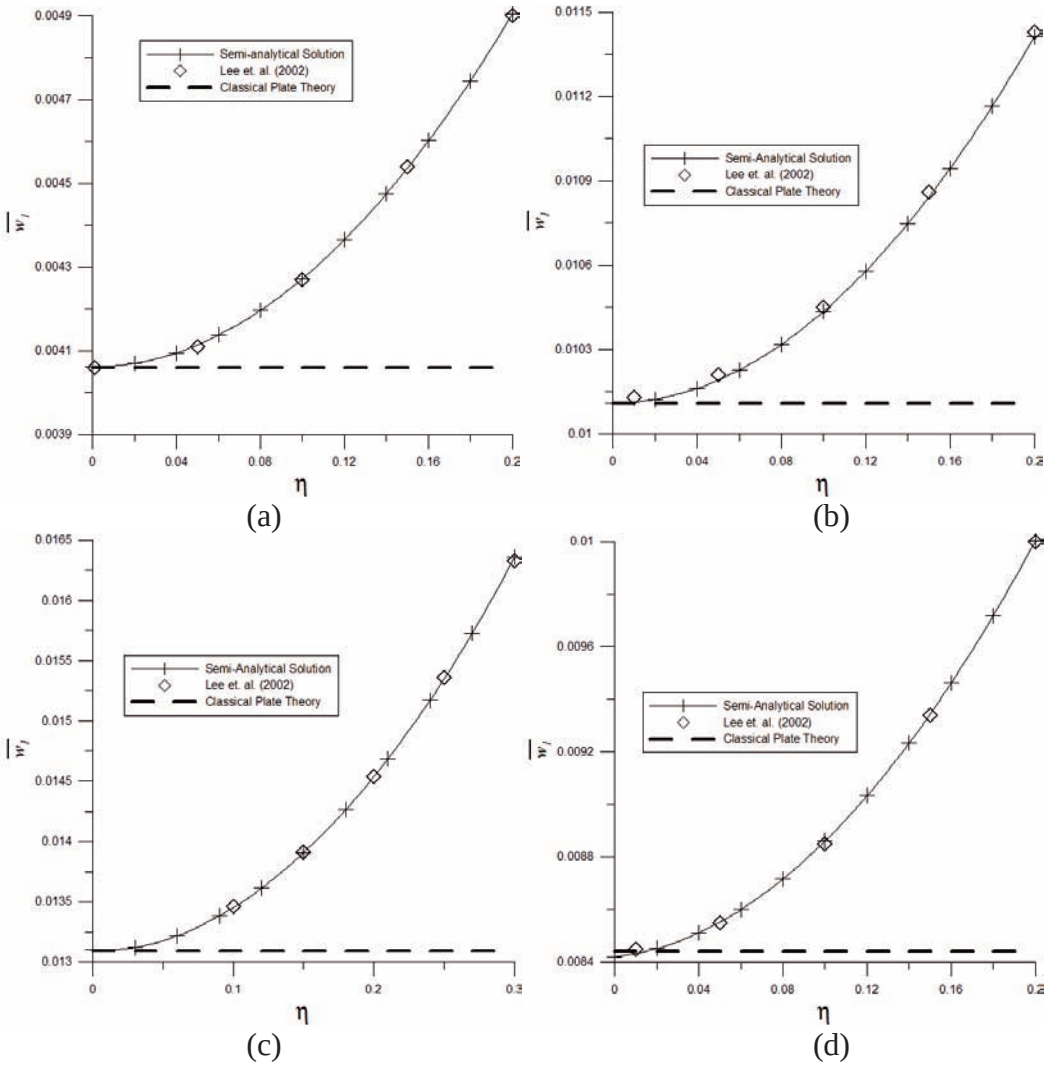

Figure 4 - Semi-analytical solutions for thick plates: (a) SSSS $a/b=1$, (b) SSSS $a/b=2$, (c) SFSF $a/b=1$ and (d) SCSC $a/b=2$

In the Table 8, it can be show that the methodology reduces to the CPT results when the thickness tends to zero. By the equation (29), the resultant term when the plate is thin is:

$$w=\frac{q_0 a^4}{D}a_1 \tag{30}$$

The solutions obtained with the present methodology can be compared with results found in the literature. The Figure 4 shows four comparisons between the equation (30), the work of Lee et. al. (2002) and the results of the CPT taken from Timoshenko and Woinowski-Krieger (1959). A good agreement between the solutions presented was achieved in thick plate

Copyright © 2010 Asociación Argentina de Mecánica Computacional http://www.amcaonline.org.ar

solutions, listed in Lee et. al. work, and in thin plate solution, found in Timoshenko and Woinowski-Krieger (1959).

SSSS				CCCC			
$a/b=1$		$a/b=2$		$a/b=1$		$a/b=2$	
a_1	TCP §	a_1	TCP §	a_1	TCP §	a_1	TCP §
0.004061	0.00406	0.010110	0.01013	0.00126	0.00126	0.00249	0.00254
SFSF				SCSC			
$a/b=1$		$a/b=2$		$a/b=1$		$a/b=2$	
a_1	TCP §	a_1	TCP §	a_1	TCP §	a_1	TCP §
0.01310	0.01309	0.21942	-	0.00193	0.00192	0.00842	0.00844

§[Timoshenko andWionowski-Krieger (1959)]

Table 8 – Degeneration of the present results to CPT results.

7. CONCLUSION

The *pb*-2 Rayleigh-Ritz method was developed and applied for the solution of rectangular shear deformable plates under transverse loading. Since the method enforces the boundary conditions through special functions which multiply the displacement interpolation functions, one can use general polynomial spaces to generate admissible solution spaces. Several cases of geometry and boundary conditions were analyzed, showing good agreement with reference solutions. The method shows a fast convergence, and is particularly suitable for benchmarking purposes. Parametric solutions for rectangular plates were generated in semi-analytic form, including the influence of the thickness.

8. REFERENCES

Craig, R. J.,1987, Finite Difference Solutions of Reissner's Plate Equations, Journal of Engineering Mechanics, vol. 113, nº 1, pp 31-48.

Kant, T., Hinton, E., 1983, "Mindlin Plate Analisys by Segmentation Method", Journal of Engineering Mechanics, vol. 109, nº 2, pp. 537-556.

Kitipornchai, S.; Xiang, Y.; Liew, K. M.; Lim, M. K., 1994, A Global Approach for Vibration of Thick Trapeziodal Plates, Computers and Structures, vol. 53, No. 1, pp. 83-92.

Lee, K. H., Lim, G. T., Wang, C. M.,2002, Thick Lévy plates re-visited, International Journal of Solids and Structures, vol. 39, nº 1, pp. 127-144.

Mindlin, R. D.,1951, Influence of Rotatory Inertia and Shear on Flexural Motions of Isotropic, Journal of Applied Mechanics, vol. 18, pp 31-38.

Salerno, V. L., Goldberg, M. A.,1960, Effect of Shear Deformations on Bending of Rectangular Plates, *Journal of Applied Mechanics*, vol. 27, pp. 54-58.

Singh, A. V., Elaghabash, Y., 2003, On finite displacement analysis of quadrangular plates, *International Jornal of Non-Linear Mechanics*, vol. 38, pp. 1149-1162.

Taylor, R. L., Govindjee, S., 2002, Solution of clamped plate problems, *Communications in numerical methods in Engineering*, vol. 20, nº 10, pp. 757-765.

Timoshenko, S. P., Woinowski-Krieger, S., 1959, *Theory of Plates and Shells*, McGraw-Hill Book Company, Auckland, 580 p.

Wang, C. M., Aung, T. M., 2007, Plastic Buckling Analysis of thick plates using p-RitzMethod, *International Journal of Solids and Strictures*, vol. 44, pp 6239-6255.

Copyright © 2010 Asociación Argentina de Mecánica Computacional http://www.amcaonline.org.ar

Wang, C. M., Lim, G. T., Reddy, J. N., Lee, K. H., 2001, Relationships between Bending Solutions of Reissner and Mindlin plate theories, *Engineering Structures*, vol. 23, pp 838-849.

Wang, C. M., Wang, Y. C., Reddy, J. N., 2002, Problems and remedy for the Ritz method in determining stress resultants of corner supported rectangular plates, *Computers and Structures*, vol. 80, pp. 145-154.

Copyright © 2010 Asociación Argentina de Mecánica Computacional http://www.amcaonline.org.ar